Materials and Structures (2026) 59:22
https://doi.org/10.1617/s11527-025-02864-x

ORIGINAL ARTICLE

Understanding bioreceptivity of concrete: realistic and accelerated weathering experiments with model subaerial biofilms

Leonie Stohl · Chiara Tonon · Jake Cook · Anna Gorbushina · Frank Dehn · Julia von Werder

Received: 30 July 2025 / Revised: 30 October 2025 / Accepted: 2 November 2025

Abstract Vertical greening systems are a promising solution to the increasing demand for urban green spaces, improving environmental quality and addressing biodiversity loss. This study facilitates the development microbially greened algal biofilm facades, which offer a low maintenance vertical green space. The study focuses on concrete as a widely used building material and explores how physical surface characteristics impact its bioreceptive properties. Concrete samples, produced from the same mix but differing in surface structure, were subjected to a laboratory weathering experiment to assess their bioreceptivity. A novel inoculation method was employed, involving a single initial inoculation with either alga (*Jaagichlorella* sp.) alone, or a model biofilm consisting of a combination of the alga (*Jaagichlorella* sp.) with a fungus (*Knufia petricola*). The samples underwent four months of weathering in a dynamic laboratory setup irrigated with deionized water to observe subaerial biofilm attachment and growth. The formation of subaerial biofilms was monitored with high resolution surface imaging, colorimetric measurements and Imaging Pulse Amplitude Modulated Fluorometry (Imaging PAM-F), with Imaging PAM-F proving the most effective. Statistical analysis revealed that by impacting surface pH value and water retention capability, surface structures significantly influence microbial growth and that the concrete's bioreceptivity can be influenced through thoughtful design of the materials surface. The inoculation of algae combined with a fungus facilitated the formation of a stable subaerial biofilm, enabling algae to colonize a surface structure that it could not colonize alone. This finding highlights the importance of modelling synergistic interactions present in natural biofilms.

Keywords Green Facades · Bioreceptivity · Concrete surfaces textures · Dynamic Laboratory Weathering · Microbial attachment · Imaging Pulse Amplitude Modulated Fluorometry (PAM-F)

L. Stohl · C. Tonon · J. Cook · A. Gorbushina · J. von Werder (✉)
Bundesanstalt Für Materialforschung und -prüfung (BAM), Unter den Eichen 87, 12205 Berlin, Germany
e-mail: julia.von-werder@bam.de

L. Stohl
e-mail: leonie.stohl@bam.de

C. Tonon
e-mail: chiara.tonon@bam.de

J. Cook
e-mail: jake.cook@bam.de

A. Gorbushina
e-mail: anna.gorbushina@bam.de

L. Stohl · F. Dehn
Institut für Massivbau und Baustofftechnologie, Baustoffe und Betonbau, Karlsruher Institut Für Technologie, Gotthard-Franz-Str., 376131 Karlsruhe, Germany
e-mail: frank.dehn@kit.edu

A. Gorbushina
Institut für Geologische Wissenschaften, Freie Universität Berlin, Malteserstr. 74-100, 12249 Berlin, Germany

Published online: 23 December 2025

1 Introduction

Ongoing urbanization [1] and deficiency of green areas in cities [2] comes with a range of problems. Without enough green spaces, mental and physical health of residents may decline [3–5] and air quality decreases [6]. Buildings are often constructed at the expense of or without sufficient compensation of green areas, which increases the urban heat island [7–9]. Moreover, overall microbial biodiversity is decreasing [10].

Vertical green spaces and green roofs are a sensible solution to the problem of lacking green spaces in urban regions [11, 12]. Greened facades can be realized with higher plants, usually implemented along with extensive irrigation and maintenance procedures. In recent years, the concept of bioreceptive materials fostering subaerial biofilm growth has gained attention as a low-maintenance alternative to traditional green facades, resulting in sustainable and self-sustaining green building envelopes [3, 13, 14].

The subaerial biofilms needed for this application are complex miniature ecosystems consisting of different types of microorganisms that are perfectly adapted for colonizing the ecological niche of artificial hard substrates [15]. Their growth is ubiquitous and inevitable [16]. Subaerial biofilms were perceived negatively for a long time [17–21], resulting in regularly repeating removal procedures and leading to loss of time, money, and in case of biocides, the release of chemicals into the environment [22]. Often this invasive cleaning of biofilms is not necessary, since they may, but don't have to damage the underlying material and often the damage is reported as mainly aesthetically unpleasant [23]. A shift in the way people perceive biofilms could pave the way for not only decreasing cleaning efforts and the use of biocides, but for using biofilms on buildings to increase green spaces in urban regions and maintain local biodiversity.

To harness the potential applications of biofilms effectively, it is crucial to understand how commonly used building materials can support and sustain the formation of desired biofilms. The material property related to this is termed bioreceptivity and was first defined by Guillitte in 1995 as the aptitude of a material to be colonized by living organisms [24] and the definition has been further elaborated in 2020 by Sanmartín et al. [23]. Bioreceptivity is a dynamic property influenced by environmental, biological, and material intrinsic factors—and over time their interactions with another. Bioreceptivity as a complex system needs further research and standardization for it to be accepted in building industry for microbially greened facades.

This study presents a step towards the construction industry with materials testing required for future application cases in mind. The focus is on concrete, a ubiquitous and widely used building material. Its versatility as artificial stone makes it specifically easy to design a material with the desired properties. As part of a holistic approach, a complementary study focuses on the material part of bioreceptivity and describes concrete sample production and material characterization fitting the context of bioreceptivity [25]. In this study, biological and environmental parameters are addressed by developing a laboratory weathering set-up which effectively tests for biological partnerships and documents biofilm formation in a defined way.

Regarding biological factors, representative microorganisms well established in subaerial biofilms must be used for meaningful bioreceptivity research, as studies showed strong difference in biofilm composition depending on the location and the type of substrate [26, 27]. The genera of the two test microorganisms—an alga and a fungus—chosen in this study are typical for local subaerial biofilm communities. The laboratory growth experiment involved samples inoculated with algae and others inoculated with a combination of both microorganisms.

To model the environment, the design of the laboratory weathering set-up is crucial. Fuentes et al. summarized the current state of commonly used laboratory set-ups as either dynamic, static, or other methods [28]. Static methods are described as horizontal storage of inoculated samples and with a water supply consisting of spraying, condensation, or capillary action. Dynamic methods are defined as weathering experiments with a sample inclination between 30° and 45° with a consistent water flow over the surface. Static set-ups are primarily suitable for assessing nutrient availability and chemical bioreceptivity of a material [29] and can be used in toxicity assessments [30]. However, physical parameters relevant for microbial attachment like porosity, roughness and water retention determined by surface structure cannot be assessed in static set-ups. Instead, a dynamic approach modeling behavior under abrasive shear stress exerted by irrigation was implemented.

For documentation of algal growth on samples, high resolution surface imaging and colour measurements widely used were implemented [13, 31–33]. In addition, Imaging Pulse Amplitude Modulated Fluorometry (Imaging PAM-F) was used to monitor the growth of photosynthetic algal cells by measuring chlorophyll fluorescence. This nondestructive method allows the monitoring of small quantities of algal cells and is particularly suitable for monitoring biofilm formation as modeled in the experiment. As the underlying substrate does not emit a fluorescence signal, the contrast between areas with and without algal cells is strong and a clear distinction can be made, making Imaging PAM-F instruments with their spatial resolution especially suited for monitoring patchy algal growth [34].

The aim of the study presented is to assess the bioreceptivity of concrete in a defined, reproducible manner for future implementation in the development of microbial greened concrete facades. The three main contributors to biocolonization: material, biology, and environment, are considered in detail and related to each other in a statistical analysis.

2 Materials and methods

2.1 Test Microorganisms

Representative organisms from the subaerial biofilm community known from façade biofilms, including species from the genera *Jaagichlorell*a and *Knufia* were chosen for this study.

The algal test microorganism *Jaagichlorella* sp. (AB13.021D5; Beck et al., in preparation) is a green coccoid alga isolated from a northwest-facing outdoor wall in Berlin-Dahlem. It was cultivated under constant shaking in liquid Bold's Basal Medium (BBM) with a 12-h light/12-h dark photoperiod and with a light intensity around ~ 100 µmol photons/m^2/s at 20 °C. Prior to the experiment, the starting culture was inoculated onto BBM agar plates at a density of 10^6 cells/cm^2 and incubated under controlled conditions (12-h light/dark cycle, 18 °C, ~ 10 µmol photons/m^2/s) for two weeks to reach the exponential growth phase.

The selected fungus *Knufia petricola* is a microcolonial black fungus known as a model representative of rock-inhabiting fungi [35–37] and for its symbiotic interaction with micro-algae [38] as well as with different mineral substrates [39, 40]. Cultivation was done at 25 °C on Malt's Extract Agar (MEA) for 7 days before being harvested.

2.2 Concrete sample preparation and inoculation

The concrete samples used in this study are made from an ultra-high performance concrete (UHPC) mix imprinted with different surface structures. The key parameters of these structures, such as arithmetic roughness, surface pH value and bioavailable water (i.e., surface-near liquid water accessible to microorganisms), are detailed in a complementary study (Table 1) [25].

Four distinct surface structures with sample dimensions of 5 cm × 10 cm were investigated (Fig. 1). An unstructured concrete surface called Blanco served as a reference surface. The surface structure Vinidur shows a grid like pattern and while exhibiting increased roughness, has a smooth and sealed off appearance similar to the reference surface Blanco. The surface structure Textile was produced through concreting on

Table 1 Surface characteristics of the differently structured concrete samples used for statistical analysis as determined in the previous publication

	Roughness [µm]	pH value after 2 h	Water sorption coefficient after 2 h [kg/(m^2*$\sqrt{h}$)]	Water uptake after 2 h [kg/m^2]	Wettability
Textile	62.38 ± 7.0	9.6 ± 0.2	0.06906 ± 0.0039	0.09767 ± 0.0055	Sorptive*
Expanded Clay	98.53 ± 23.9	10.6 ± 0.4	0.04172 ± 0.0026	0.05900 ± 0.0036	Sorptive*
Vinidur	65.92 ± 25.6	10.4 ± 0.4	0.01862 ± 0.0046	0.02633 ± 0.0065	Hydrophilic**
Blanco	25.53 ± 8.5	9.9 ± 0.1	0.01556 ± 0.0043	0.02200 ± 0.0061	Hydrophilic**

The material properties (arithmetic) roughness, pH value of distilled water in contact with the concrete surface for 2 h, capillary water sorption coefficient and water uptake after 2 h adapted from DIN EN 13057, and wettability derived from water contact angles (*sorptive: material absorbs water droplets placed; **hydrophilic exhibits a water contact angle below 90°) are presented

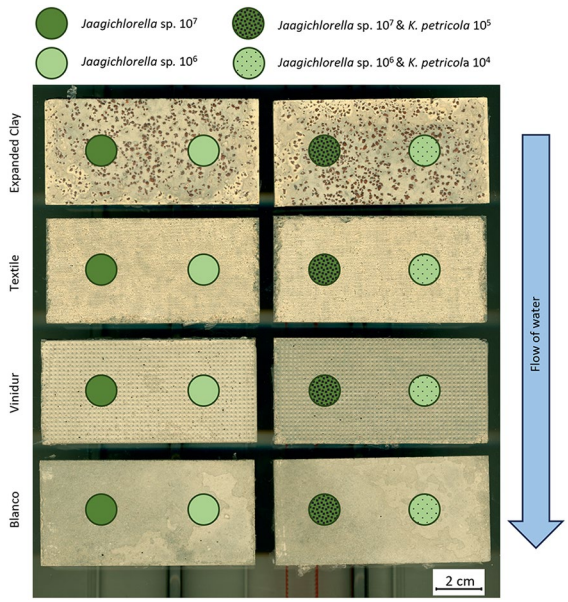

Fig. 1 Scheme of concrete samples inoculated with different concentrations and types of microorganisms. Differently structured concrete samples (5 cm × 10 cm, top to bottom: Expanded Clay, Textile, Vinidur, Blanco) were tested with two concentrations of either algal inoculation (left) or a combination of algal + fungal inoculation (right). Placing the droplets containing microorganisms next to another ensured no interaction between the inoculations due to water run-off. Droplets are not to scale, and the color intensity is exaggerated for illustration purposes

a textile and ripping it out of the material after hardening, leading to a sorptive and porous surface. The fourth surface structure Expanded Clay was produced through adding expanded clay aggregates onto the hardening concrete, leading to a surface with mixed surface properties combining those of the aggregates and those of the unstructured concrete surface.

For the laboratory growth experiments, these differently structured concrete samples were sterilized in an autoclave and then put on agar in Petri dishes to maintain stable humidity. To enhance algal attachment, surfaces were pre-coated with 4 × concentrated, liquid algal media (BBM, 88.4 µL/cm^2) before inoculation.

The biomass for inoculation was harvested from plates and suspended in liquid. Desired concentrations were achieved via cell counting. The growth experiment involved two types of inoculation: one with only algal cells and the other with a mixed inoculation of algae and fungi. For the algal inoculation, each sample was inoculated with 10 µL of *Jaagichlorella* sp. suspension. Two droplets, each with different concentrations (10^6 and 10^7 cells/ml), were applied to each sample. The mixed inoculation included both *Jaagichlorella* sp. (10^6 and 10^7 cells/ml) and *K. petricola* (10^4 and 10^5 cells/ml, respectively) to assess potential microbial interactions on the different surface structures. The droplets were placed side by side to ensure that the inoculations did not interact (Fig. 1). Prior to subjecting the inoculated concrete samples to laboratory weathering, the microorganisms underwent a 2-day acclimation period to facilitate a smoother transition from the ideal culturing conditions to the weathering conditions.

The bioreceptive performance of the four concrete surface structures was assessed in triplicate. In case of the algal inoculation, three samples per surface structure were inoculated with two different algal concentrations each, leading up to a total of six inoculations per surface structure. Considering all four surface structures, a total of 12 samples with 24 inoculations was tested. The same protocol was followed for the mixed inoculation, adding a total of another 12 samples with 24 inoculations.

2.3 Accelerated weathering laboratory set-up

The laboratory set-up was adapted from Barberousse [27] and employed a dynamic design with a sample inclination of 45°. Two identical weathering chambers were constructed, one for testing samples with algal inoculation and one for testing samples with mixed inoculation. Within each set-up, the samples were distributed randomly to ensure unbiased conditions.

Both set-ups consisted of custom-built PVC-boxes, measuring 75 cm × 61 cm × 61 cm (W x H x D). Each box had a drainage hole in the base to facilitate water outflow and was equipped with 5 cm long feet to ensure unrestricted drainage (Fig. 2).

Perforated stainless steel sheets, each measuring 50 cm × 72 cm, were prepared for the set-up. The sheets were separated by 30.5 cm long spacers, creating a structured arrangement. The lower sheet was used for sample placement, while the upper sheet was designated for mounting the lighting system. Nine LED arrays (eco + LED bar PLANT-GROW, LEDaquaristik GmbH, Germany) were installed onto the perforated metal sheet and the light intensity set

with a control unit (SimuLUX 24 dimming control and daylight simulation, LEDaquaristik GmbH, Germany) and the corresponding software (SimuLUX 24 software, LEDaquaristik GmbH, Germany), allowing to adjust every LED array individually. Lighting was set to a homogeneous intensity of 3.8 µmol/m^2/s, matching the conditions used for algal cultivation. To minimize external light interference and further enhance lighting uniformity, the weathering set-ups were wrapped in alumina foil. The light intensity was measured and verified using a light sensor (FLA 623 PS, Ahlborn GmbH, Germany) and a 12 h light/12 h dark cycle was implemented.

The irrigation system consisted of an outdoor cooling mist set-up (Outdoor Cooling Mist Set 13,135, Gardena GmbH, Germany) connected to a timer (Water Control Master 1892, Gardena GmbH, Germany). It was programmed to operate during the 12-h daytime period, delivering 1 min of irrigation every 3 h. Deionized water was used throughout the experiment.

Humidity was regulated using a humidity sensor (TMT-HC-210 Humidity Control II, Import Export Peter Hoch GmbH, Germany), connected to a humidifier (SuperFog II, Import Export Peter Hoch GmbH, Germany). The system was set to maintain a minimum relative humidity (rH) of 80% during the day and 90% during the night.

To ensure consistent conditions, both set-ups were equipped with an additional sensor to monitor humidity and temperature (FHAD 46-C2, Ahlborn GmbH, Germany). Data was taken once every 10 min and recorded by a compatible datalogger (Almemo 2890–9, Ahlborn GmbH, Germany). The average temperature recorded was 21.6 ± 1.3 °C.

2.4 Growth monitoring

All documentations were taken through the Petri dish lid. High resolution surface imaging was performed using an office scanner with a resolution of 800 ppi (Scanmaker 1000 XL Plus, Mikrotek, Taiwan). Color measurements were carried out using a handheld spectrophotometer (Ci62L, X-Rite, USA) equipped with a 14 mm aperture and a respective measurement area of 1.54 cm^2. Results were recorded as L*a*b values and managed in the corresponding software (Color iQC Professional, X-Rite, USA). The L*a*b color space is designed to approximate human vision. It consists of three axes: L for lightness, a for the green–red spectrum, and b for the blue-yellow spectrum.

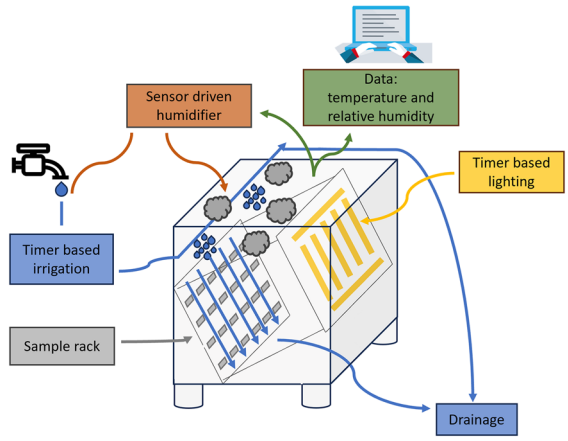

Fig. 2 Schematic of one laboratory weathering chamber. A dynamic approach with a sample inclination of 45° and a mist cooling irrigation system was implemented. LED arrays ensured uniform lighting and implement a 12 h/12 h day/night cycle. Relative humidity was controlled by a sensor-based humidifier. Temperature and relative humidity were recorded by additional sensors

For Imaging PAM-F measurements, a MINI version of the IMAGING-PAM M series (Heinz Walz GmbH, Effeltrich, Germany) with a blue measuring head (IMAG-MIN/B) and a measurement are of 24 × 32 mm was used. The corresponding software ImagingWin v2.56zn was used for data collection and processing. Prior to measurement, the samples were dark adapted for 20 min and then measured with the same measurement setting (Saturation pulse 1, Measuring light 3, Gain 1). The recorded base chlorophyll fluorescence F_0 value was used as a marker for biomass, with the maximum F_0 signal (= F_0-max) providing point-specific information about the highest signal recorded on a sample. Due to the low biomass on the materials, the F_0-max in this study could be correlated with the maximum biomass accumulation and, consequently, with the thickness of the algal cover on a sample. Additionally, the visual representation of measurements (Fig. 4) was analyzed in ImageJ to quantify the percentage of the measurement area covered by the F_0 chlorophyll fluorescence and hence algal cells (= F_0-area). This involved converting images to grayscale and transforming them into binary files. To reduce noise, a minimum area

threshold of 15 pixels was applied before calculating the percentage of the area displaying chlorophyll fluorescence.

Initial documentation was performed after inoculation and drying of the droplets. After the 2 day acclimation period the samples were transferred to the laboratory weathering set-up. Samples were removed from the set-up after 9, 20, 49, 84, and 112 days, allowed to dry, and measured again in their Petri dishes before being returned to the weathering chamber. To ensure consistency in measurements, samples were removed from the set-up at the same time and dried for a specified period. Variations in wetness can affect the results, with moist surfaces leading to darker values for the lightness parameter during the colorimetric measurements and potentially higher noise or fluorescence values in Imaging-PAM-F measurements. Some residual moisture should be maintained, especially if additional insights into cell health or photosynthetic efficiency are needed from Imaging- PAM-F data. Data visualization was done in Origin (V. 2022, OriginLab Corporation, USA).

2.5 Statistical analysis

All statistical analyses were performed using R Statistical software (V. 4.4.1, R Core Team 2024). A three-way ANOVA was conducted with the log-transformed F_0-area values after 112 days as the dependent variable, and microorganism type, concentration, and surface structure as the independent variables. To determine significant differences between groups, an interaction test was conducted followed by a post-hoc Tukey test, with statistical significance set at $p \leq 0.05$.

A correlation analysis between the material parameters and F_0-area was carried out to fully include the material aspect of biocolonization (Table 1).

3 Results

3.1 Growth monitoring

Biological growth was defined differently for each method implemented. In case of high resolution surface imaging, growth was defined as being able to detect a visual staining on the concrete surfaces, while for colorimetric measurements, a recorded color change may be attributed to biological growth. Algal growth measured in the Imaging PAM-F was monitored by either an increase in a F_0-max or an increase in F_0-area. The effectiveness and suitability of the documentation methods was compared and is presented in Table 2.

High resolution surface images taken throughout the experiment were evaluated visually and showed microbial growth as light green staining the earliest on day 49, more noticeable starting from day 84 (Table 2). The surface structures Textile and Expanded Clay showed visible greening, however, the contrast between concrete and the subtle green patches of starting algal growth was insufficient for meaningful analysis and data was not processed further.

The colorimetric data showed a pattern consistent with the high resolution surface imaging results. While color changes were documented, they were subtle and could not be reliably attributed to algal growth. The Δa values, which would indicate a shift towards green, showed only minimal changes (Fig. 3). Blanco and Vinidur showed no growth, which agrees well with findings of the high resolution

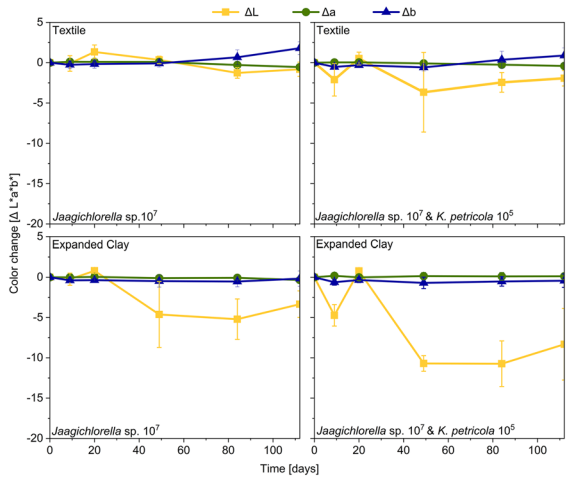

Fig. 3 Representative colorimetric data for the two out of four surface structures showing visible greening in surface imaging. Data corresponds to high-concentration inoculations, with Textile depicted in the upper row and Expanded Clay in the lower row. Left column: algal inoculation (10^7); right column: combined algal (10^7) and fungal (10^5) inoculation. Despite algal growth being visible in surface imaging, no shift towards green (-Δa) was observed. Fungal growth was slightly visible, with samples inoculated with *K. petricola* exhibiting more pronounced darkening (-ΔL). Surface structures Blanco and Vinidur are excluded as they showed no visible greening in surface images

Table 2 Comparison of documentation methods used to monitor algal growth on concrete samples over time (Day 9 – Day 112)

		High concentration (10^7 algal cells/ml or 10^7 algal cells/ml + 10^5 fungal cells/ml)										Low Concentration(10^6 algal cells/ml or 10^6 algal cells/ml + 10^4 fungal cells/ml)									
		Day 9		Day 20		Day 49		Day 84		Day 112		Day 9		Day 20		Day 49		Day 84		Day 112	
		F_0	Images	F_0	Images	F_0	Images	F_0	Images	F_0	Images	F_0	Images	F_0	Images	F_0	Images	F_0	Images	F_0	Images
Jaagichlorella sp.	Blanco_01	×	×	×	×	×	×	×	×	×	×	×	×	×	×	×	×	×	×	×	×
	Blanco_02	×	×	×	×	×	×	×	×	×	×	×	×	×	×	×	×	×	×	×	×
	Blanco_03	×	×	×	×	×	×	×	×	×	×	×	×	×	×	×	×	×	×	×	×
	E. Clay_01	×	×	×	×	✓	×	✓	✓	✓	✓	×	×	✓	×	✓	×	✓	×	✓	✓
	E. Clay_02	✓	×	✓	×	✓	×	✓	✓	✓	✓	×	×	×	×	✓	×	✓	×	✓	✓
	E. Clay_03	×	×	×	×	✓	×	×	×	×	×	✓	×	✓	×	×	×	×	×	×	×
	Textile_01	×	×	×	×	✓	×	✓	✓	✓	✓	×	×	×	×	✓	✓	✓	✓	✓	✓
	Textile_02	✓	×	✓	×	✓	×	✓	✓	✓	✓	×	×	×	×	✓	✓	✓	✓	✓	✓
	Textile_03	×	×	✓	×	✓	×	✓	✓	✓	✓	×	×	×	×	✓	×	✓	✓	✓	✓
	Vinidur_01	×	×	✓	×	×	×	×	×	×	×	×	×	×	×	×	×	×	×	×	×
	Vinidur_02	×	×	×	×	×	×	×	×	×	×	×	×	×	×	×	×	×	×	✓	×
	Vinidur_03	×	×	✓	×	×	×	×	×	×	×	×	×	×	×	×	×	×	×	×	×
Jaagichlorella sp. & *K. petricola*	Blanco_01	×	×	×	×	×	×	×	×	×	×	×	×	×	×	×	×	×	×	×	×
	Blanco_02	×	×	×	×	×	×	×	×	×	×	×	×	×	×	×	×	×	×	✓	×
	Blanco_03	×	×	×	×	×	×	×	×	×	×	×	×	×	×	×	×	×	×	×	×
	E. Clay_01	×	×	×	×	×	×	×	×	✓	×	×	×	✓	×	×	×	×	×	✓	×
	E. Clay_02	×	×	×	×	×	×	×	×	✓	×	×	×	✓	×	×	×	×	×	✓	×
	E. Clay_03	×	×	×	×	×	×	✓	✓	✓	✓	×	×	×	×	×	×	×	×	✓	×
	Textile_01	×	×	×	×	✓	×	✓	✓	✓	✓	×	×	✓	×	✓	×	✓	×	✓	✓
	Textile_02	×	×	×	×	✓	×	✓	✓	✓	✓	×	×	×	×	✓	×	✓	✓	✓	✓
	Textile_03	✓	×	✓	×	✓	×	✓	✓	✓	✓	×	×	✓	×	✓	×	✓	✓	✓	✓
	Vinidur_01	×	×	✓	×	✓	×	✓	✓	✓	✓	×	×	×	×	✓	×	✓	✓	✓	✓
	Vinidur_02	×	×	✓	×	×	×	✓	✓	✓	×	×	×	×	×	×	×	×	×	×	×
	Vinidur_03	✓	×	✓	×	✓	×	✓	×	✓	×	×	×	✓	×	✓	×	✓	×	✓	×

The tested methods included high-resolution surface imaging (Image), Imaging PAM-F (F_0), and colorimetry (not shown). For each combination of inoculation concentration (high or low), microorganism type (algae or algae + fungi), and concrete surface structure (Blanco, E. Clay, Textile, Vinidur), all replicates are shown. Algal growth was defined as either visible green coloration in surface images or detection of an F_0 signal with Imaging PAM-F. Colorimetric measurements were excluded, as they did not reliably document algal growth (i.e., a shift toward the green range). A check mark (✓) indicates chlorophyll fluorescence was observed, while a cross (×) indicates no chlorophyll fluorescence

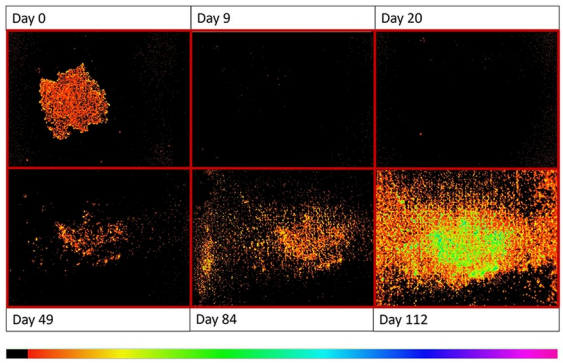

Fig. 4 Algal growth as chlorophyll fluorescence (F_0) images obtained by Imaging PAM-F on an exemplary concrete sample with Textile structure. Images show an initial chlorophyll fluorescence after inoculation with *Jaagichlorella* sp. (10^7 cells) on day 0 with a strong decrease on day 9 and 20 after being exposed to irrigation cycles in the laboratory weathering set-up. Following an initial, sample-dependent period with little or no observable growth, bioreceptive samples begin to show growth in later stages. The fluorescence signal follows the surface structure, showing algal interaction and growth on the surface rather than mere accumulation

surface imaging (Table 2). However, in case of Textile and Expanded Clay, which visibly turned green in the high resolution surface images, this means algal growth was not properly assessed with colorimetric measurements, even in case of the high concentration inoculations. The most significant variation was observed in the ΔL value (lightness), which was especially pronounced for mixed inoculations (Fig. 3).

Imaging PAM-F detected algal presence early on (Table 2) and allowed for a close-up monitoring over time. Figure 4 provides an example of the general growth trend observed on the samples that developed algal biomass by the end of the experiment. The Imaging PAM-F clearly captures the chlorophyll fluorescence from the initial inoculation (day 0). After being placed in the laboratory weathering set-up and exposed to the irrigation system, chlorophyll fluorescence is drastically reduced for the next documentation points (day 9 and day 20). Bioreceptive samples initially showed no algal presence, but after a sample-specific period, growth became apparent and followed the surface structure. Comparing the impact of the two different inoculation concentrations on algal growth, higher initial concentrations of algal cells generally resulted in higher F_0-max values over time. This trend was observed primarily for surface structures that exhibited growth visually discernible algal growth (Fig. 5). A similar pattern can be seen comparing the type of microorganism inoculated, with samples containing the fungus in addition to the alga producing lower F_0-max readings than samples inoculated only with alga. For Expanded Clay textures

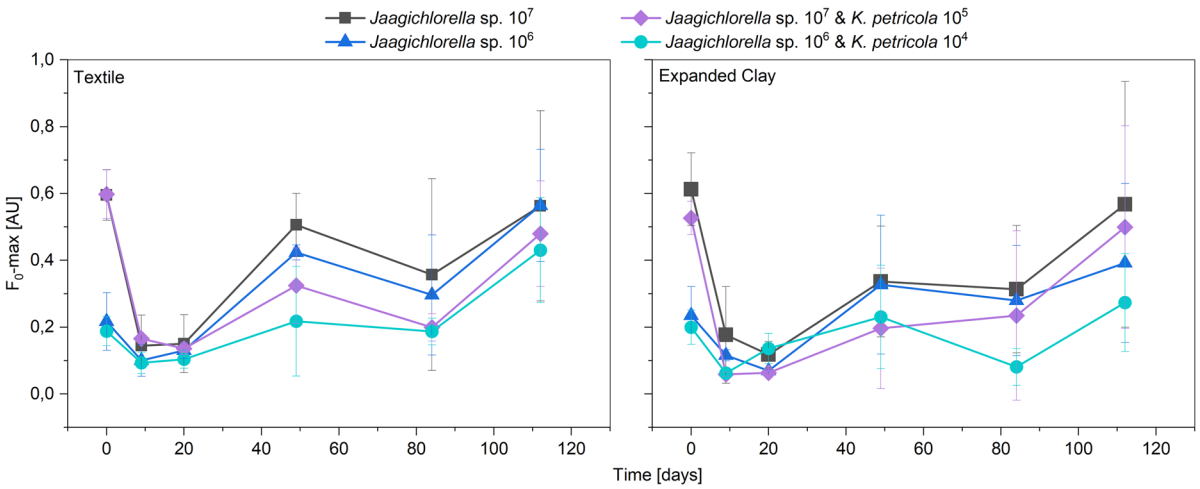

Fig. 5 Maximum base chlorophyll fluorescence F_0-max detected by Imaging PAM-F for the two out of four surface structures visually exhibiting growth in the high resolution surface images (Left: Textile; Right: Expanded Clay) and for every combination of concentration and microorganism type over time. F_0-max relates to the highest signal intensity measured and correlates to the maximum biomass accumulation present on a sample. Higher inoculation concentration leads to higher F_0-max values recorded, however both inoculation concentrations were sufficient to promote growth. Inoculations containing algae and fungi generally produced lower F_0-max values than the same samples inoculated without fungi

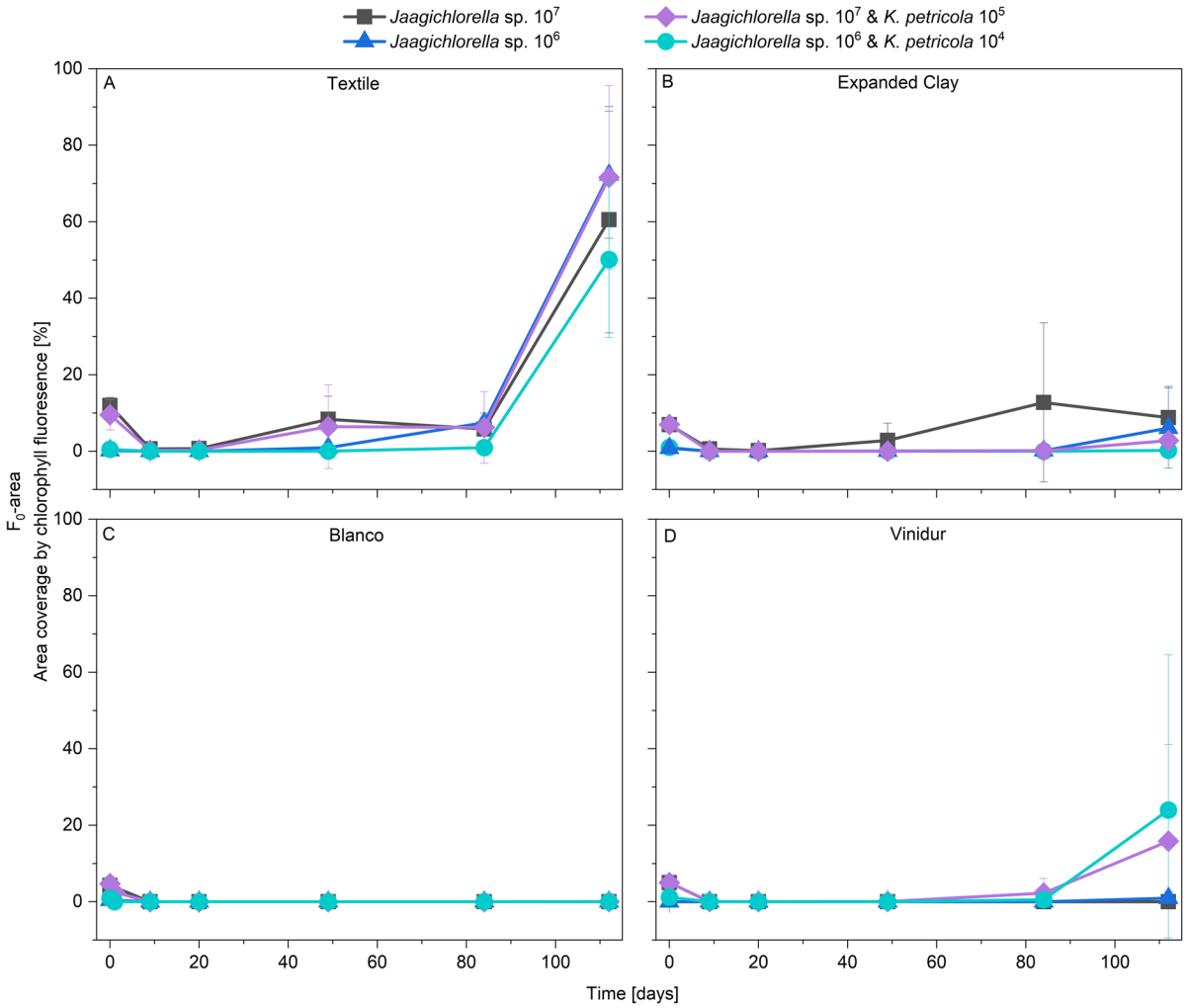

Fig. 6 Growth as F_0-area coverage on the differently structured concrete samples over 4 months. F_0-area coverage (%) was calculated from the F_0 value collected by Imagining PAM-F data further processed in ImageJ. Graphs show F_0-area values over time for both inoculation concentrations and both microorganism types on all surface structures, Textile (A), Expanded Clay (B), Blanco (C) and Vinidur (D). The Textile structure shows comparable growth in all scenarios, while Expanded Clay shows lower F_0 area coverage with *K. petricola* present. The Vinidur structure shows improved bioreceptivity when *K. petricola* was present. The reference surface Blanco does not exhibit growth

this trend is reversed in the early stages (day 20, day 49), where the lower inoculation concentration containing both microorganisms scores higher F_0-max values than the high inoculation (Fig. 5).

Results further show that after 112 days all concrete samples with the Textile structure exhibit growth in varying intensity with both types of microorganisms and inoculation concentrations, leading to algal growth in 12 out of 12 inoculations. Concrete samples with expanded clay aggregates on their surface showed growth on two out of three samples inoculated with *Jaagichlorella* sp., and in all three samples inoculated with a combination of *Jaagichlorella* sp. and *K. petricola*, regardless of inoculation concentration. This led to growth in 10 out of 12 cases, demonstrating a consistent response in samples with this surface structure. However, the growth pattern is highly variable and especially with *K. petricola* present, only small specks of chlorophyl fluorescence were measured and counted as growth (Appendix—Table 4, Table 5).

Concrete samples with the Vinidur structure inoculated with *Jaagichlorella* sp. show growth on

only one sample at a low inoculation concentration, indicating that the likelihood of algal growth on this surface is quite low, as growth only happened in one out of six potential cases. When *K. petricola* was included, two out of three samples showed growth regardless of the inoculation concentration, resulting in four out of possible six cases exhibiting growth. Growth was primarily observed on the raised ridges, indicating the importance of surface topography (Appendix—Table 4, Table 5).

In contrast, the non-structured Blanco samples showed no significant biological growth, and the recorded value on one sample is likely due to measurement noise (Appendix—Table 4, Table 5).

Focusing on the influence of the type of microorganism, inoculation with *Jaagichlorella* sp. alone led to growth on 5 out of 12 samples and a total of 11 out of 24 inoculations exhibited growth.

When inoculated with *Jaagichlorella* sp. and *K. petricola*, a total of 16 out of 24 inoculations showed growth. These results strongly indicate that the presence of *K. petricola* enables better subaerial biofilm attachment, especially on the Vinidur structure.

Combining the F_0-max value with spatial information offers valuable insights in biofilm development. For utilizing the spatial information provided by the Imaging PAM-F images, chlorophyll fluorescence images were further processed in ImageJ to obtain the algal growth as F_0-area (Fig. 6). After an initial delay, algal growth measured as F_0-area occurs on the concrete samples with Textile, Expanded Clay, and Vinidur surfaces. After four months of laboratory weathering, the Textile surface records the highest F_0-area values, and the results are comparable for all test scenarios. Expanded Clay shows lower F_0-area values when inoculated with a mix of microorganisms compared to an only algal inoculation, whereas Vinidur performs significantly better with *K. petricola*. The reference structure Blanco did not show growth.

While high resolution surface imaging and colorimetric data offered limited insights, Imaging PAM-F allowed a precise monitoring of the algal growth on the samples. Differences between the microorganisms and inoculation concentrations could be observed and the different surface structures led to varying biological growth.

3.2 Statistical analysis

Tests for normal distribution ($p = 0.11$) and homogeneity of variances ($p = 0.85$) confirmed that the assumptions for ANOVA were met. The results of the conducted ANOVA (Table 3) show that surface structure was a highly significant factor ($p < 0.01$), for spatial algal growth (F_0-area) and that the microorganism type (Organism) had a significant effect ($p = 0.03$). The inoculation concentration did not show a significant influence ($p = 0.81$).

Partial ETA^2 (ηp^2) values indicated that surface structure had the largest effect on F_0-area ($\eta p^2 = 0.60$), whereas organism type had a moderate effect ($\eta p^2 = 0.15$). Concentration and the interaction terms showed minimal effects ($\eta p^2 < 0.05$ in all cases).

Post-hoc analyses (Table 3) confirmed the variable Organism as significant, with the combination of *Jaagichlorella* sp. and *K. petricola* (emmean = —6.46) outperforming *Jaagichlorella* sp. (emmean = −9.72).Although concentration was not identified as a significant factor, the results suggest a slightly better performance of the high concentration (emmean = -7.92) compared to the lower concentration (emmean = −8.26). The results for the different surface structures indicated that Blanco (emmean = −14.07) was the least bioreceptive, followed by Vinidur (emmean = −9.51), Expanded Clay (emmean = −8.27), and Textile (emmean = −0.52), which exhibited the highest bioreceptivity.

Pairwise post-hoc comparisons (Table 3) showed no significant differences between Blanco and Vinidur nor between Vinidur and Expanded Clay but were significant for all remaining comparisons. Carrying out this three-factor ANOVA with the variable surface structure substituted by either pH value after 2 h, water retention after 2 h, or roughness (Table 1) yields the same results, which can be explained by the material being an independent and highly significant factor.

The correlation matrix (Fig. 7) investigated the relations between the material intrinsic parameters that, together, define each a surface structure. The results suggest limited multicollinearity among the independent variables and but also show correlations between the parameters exist. Moderate positive correlations between roughness and pH after 2 h ($r = 0.65$) and weak positive correlations between

Table 3 ANOVA results for the dependent variable spatial algal growth after 4 months (F_0-area), including partial ETA^2 (ηp^2) and post-hoc analyses. The independent factors (Surface structure, Organism, and Concentration) showed varying levels of significance, with Surface structure being highly significant and exhibiting the largest ηp^2. Post-hoc results indicate differences between the levels of the significant variables Surface structure and Organism type. Post-hoc pairing effectively compared the bioreceptivity of the different Surface structures

ANOVA		
Factor	*p*-value	
Surface structure	> 0.00	
Organism	0.03	
Concentration	0.81	
Surface structure:Organisms	0.26	
Surface structure:Concentration	0.84	
Organisms:Concentration	0.74	
Surface structure:Organisms: Concentration	0.76	
Partial ETA^2		
Parameter	ηp^2	95% CI
Surface structure	0.60	[0.40, 1.00]
Organisms	0.15	[0.01, 1.00]
Concentration	0.00	[0.00, 1.00]
Surface structure:Organisms	0.12	[0.00, 1.00]
Surface structure:Concentration	0.03	[0.00, 1.00]
Organisms:Concentration	0.00	[0.00, 1.00]
Surfacestructure:Organisms: Concentration		
Concentration	0.04	[0.00, 1.00]
Post-hoc		
Grouped Factors	emmean	95% CI
Organisms		
Jaagichlorella sp.	−9.72	[−11.73, −7.71]
Jaagichlorella sp. with *K. petricola*	−6.46	[−8.47, -4.45]
Concentration		
Low inoculation concentration	−8.26	[−10.27, −6.25]
High inoculation concentration	−7.92	[−9.93, −5.91]
Surface structure		
Blanco	−14.07	[−16.91, −11.23]
Expanded Clay	−8.27	[−11.11, −5.42]
Textile	−0.52	[−3.36, 2.33]
Vinidur	−9.51	[−12.35, −6.67]
Post-hoc pairing		
Pairwise comparison	emmean	p-value
Blanco—Expanded Clay	−5.80	0.03
Blanco—Textile	−13.55	0.00
Blanco—Vinidur	−4.56	0.12
Expanded Clay—Textile	−7.75	0.00
Expanded Clay—Vinidur	1.24	0.92
Textile—Vinidur	8.99	0.00

roughness and water retention after 2 h (r = 0.40) were calculated. In contrast, pH after 2 h and water retention after 2 h exhibit a moderate negative correlation (*r* = —0.44).

Looking at the correlation between independent and dependent variables, the strongest correlation with F_0-area is observed for water retention after 2 h (r = 0.62). The pH value after 2 h shows a moderate negative correlation (*r* = −0.49), suggesting that higher pH values may reduce F_0-area coverage, while roughness has a negligible correlation (*r* = 0.04), implying minimal direct influence.

In conclusion, surface structure was the most significant variable influencing the spatial algal growth recorded after four months (F_0-area), followed by Organism with a moderate effect, while concentration showed negligible influence. Looking at the surface characteristics, water retention after 2 h proved to be the most influential parameter. Among the surfaces, Textile demonstrated the highest bioreceptivity.

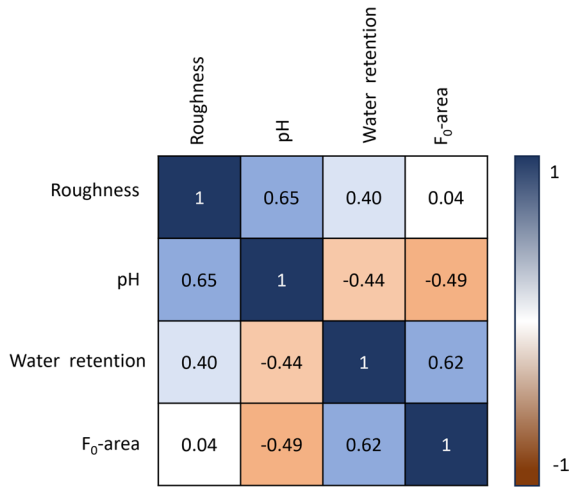

Fig. 7 Pearson correlation matrix for intrinsic surface parameters (Roughness, pH, Water retention) and F_0-area (spatial algal growth after 4 months). Positive and negative correlations indicate the direction of the relationship, with stronger correlations representing greater association between variables

4 Discussion

This study presents a laboratory weathering setup designed to assess the influence of different concrete surface structures on biological growth. The dynamic setup (Fig. 2) features multiple short wetting periods per day (5 × 1 min) using deionized water coupled with inclined sample positioning. While driving rain is an important water source for biofilms [41], recent research has highlighted the importance of dew and prolonged drizzle as significant sources of moisture, compared to short-term rain events [42, 43]. The mist cooling system used in this study dispersed water into finer droplets than those typically produced by conventional irrigation systems, effectively simulating relevant natural moisture sources. Moreover, mist cooling systems are commonly used in warmer regions to cool urban environments, and their use is expected to spread to other areas [44]. These systems may offer a dual benefit as efficient, water saving irrigation systems for microbially greened façades.

In comparable studies, samples are often irrigated twice daily for 60–90 min using nutrient-rich media or algal suspensions [13, 18, 27, 32, 33]. Such methods can introduce artificially high nutrient levels and may favor cell accumulation over biofilm attachment and formation. However, the most crucial and time-consuming phase of natural biofilm growth is usually the initial, reversible attachment stage that precedes irreversible adhesion [45] and it is essential that laboratory weathering experiments capture this process.

To ensure realistic conditions for biofilm development, samples were inoculated only once at the beginning of the experiment (Fig. 1). Surface-dependent algal colonization was monitored throughout the study, with increased documentation frequency in the beginning of the experiment to capture early attachment dynamics. Microorganisms were detectable on the surfaces immediately after inoculation but were absent during the subsequent measurement periods, reemerging later and spreading across a broader area (Paragraph 3.1; Fig. 4). This shows an active interaction between the biofilm and the substrate, indicating genuine biological attachment and growth rather than passive accumulation. These results confirm that the experimental setup successfully captured the critical stages of microbial attachment and biofilm formation.

Selecting robust, representative, and symbiotically competent species for bioreceptivity testing is essential. In this study, two inoculation strategies were evaluated: the microalga *Jaagichlorella* sp. alone, and in combination with the fungus *K. petricola*. While using a single strain simplifies the model, introducing a dual strain approach including both phototroph and heterotroph microorganisms can capture synergistic interactions between different groups of microorganisms [16, 28].

The presence of *K. petricola* affected colonization success. One surface type (Vinidur) was preferentially colonized by algal cells when the fungus was present (Table 2), underscoring the symbiotic dynamics typical of natural biofilms. The combination of both organisms creates a model biofilm relevant to sun- and air-exposed surfaces, supporting reproducible and accelerated testing of biogenic effects. This development facilitates the study of biodeterioration as well as the optimization of material formulations for innovative, microbially greened façades for innovative microbially greened algal facades [46].

Despite their widespread use in similar set-ups [13, 31–33], high resolution surface images and colorimetric measurements proved insufficiently sensitive for reliably monitoring biomass development in this study. The inoculation chosen in terms of algal strain and cell numbers resulted only in a very light coloration, coupled with a thin and patchy distribution of growth. Colorimetric measurements refer to a standard observer and are therefore not more sensitive than the human eye or the high resolution surface images. Due to the contrast between melanized black fungi and grey concrete, differences in lightness between inoculations with and without the fungus could be detected (Fig. 3). However, it should be noted that varying humidity levels also influence colorimetric measurements. Neither colorimetric analysis nor surface imaging were able to detect algal growth effectively. In contrast, Imaging PAM-F provided reliable detection below the visibility threshold and proved highly effective for tracking low algal concentrations over time (Table 2).

Imaging PAM-F data was used for its spatial information (F_0-area, Fig. 6) and measure of local maximum of algal biomass accumulation (F_0-max, Fig. 5). As Imaging PAM-F measures chlorophyll fluorescence, it only detects algal cells and cannot monitor the presence of the fungus. Moreover, a buildup of algal layers, the presence of the fungus or the

substrates' structure itself may lead to shading effects, underestimating algal biomass, and complicating direct comparisons between single and dual inoculations. Reduced F_0-max values observed in the presence of *K. petricola* (Fig. 5) may be partially attributed to fungal shading rather than only to differences in algal biomass development. Spatial imaging further revealed growth patterns along surface structures and highlighted substantial variability in colonization (Appendix—Table 4, Table 5), which is typical and within the limits for biological experiments.

Among the tested methods, Imaging PAM-F was the only technique capable of reliably documenting the critical initial stages of biofilm formation and should be more widely adopted in bioreceptivity research.

A three-way ANOVA was conducted to evaluate the influence of inoculation concentration, microorganism type, and concrete surface structure on algal coverage, expressed as F_0-area at the end of the experiment. This metric incorporates spatial distribution and accounts for the observed variability in growth patterns (Paragraph 3.1, Appendix—Table 4, Table 5). Surface structure emerged as the most significant factor (Table 3), and material properties (Table 1) from a previous study [25] were linked to the ANOVA results for further interpretation.

The non-structured reference surface (Blanco), featuring minimal water retention and smooth structure, lacked attachment points for microbial growth. Consequently, the irrigation system washed off the inoculated biomass, and no growth was observed on this surface (Fig. 6). Vinidur, although similar in smoothness, featured a grid-like imprint with defined roughness but limited porosity. Algal colonization was more successful when *K. petricola* was present, suggesting a synergistic effect that enhanced attachment (Fig. 6).

The Expanded Clay surface incorporated aggregates with lower pH and higher water retention than surrounding concrete, creating a potentially favorable environment for biofilm formation. However, algal growth did not preferentially occur on the aggregates, likely because the initial inoculation was applied to the concrete surface. The aggregates appeared to influence water flow, reducing wash-off and favoring attachment. Algae were likely transported by water and deposited within porous, chlorophyll-shading aggregates, from which they subsequently grew outward, resulting in the appearance of growth surrounding the aggregates (Appendix—Table 4, Table 5). The Textile surface structure, characterized by the highest water retention and porosity, proved to be the most bioreceptive.

Microorganism type (Organism) was also identified as a significant factor (Table 3). Lower chlorophyll fluorescence values were recorded in the presence of *K. petricola*, likely due to fungal shading rather than inhibited algal growth. This effect was supported by darker colorimetric values (Fig. 3) and reduced F_0-max readings (Fig. 5), although no consistent trend was observed in F_0-area values (Fig. 6). On highly bioreceptive surfaces like Textile, shading effects were negligible, while on less receptive surfaces like Expanded Clay, a decline in F_0-area was observed with fungal presence.

More importantly, especially for the ANOVA, more samples were colonized when *K. petricola* was present (Table 2). In comparison to algae, fungi can penetrate and quickly spread over the substrate [47], thus establishing contacts to the substrate and anchoring the biofilm [15, 16]. The improved survival rate and spatial colonization F_0-area of *Jaagichlorella* sp. combined with K. petricola on the Vinidur surface suggests that the approach of developing a model biofilm is effective, enabling the test microorganisms to successfully attach. It can therefore be assumed that in this case the fungus does not hinder algal growth but supports it. This result highlights the potential for leveraging synergistic interactions, commonly observed in natural biofilms.

Inoculation concentration showed no significant influence in case of the two tested concentrations, both concentrations chosen were able to develop biomass. However, below a certain minimum concentration needed for growth, an influence of the concentration would be clearly recognisable and significant.

Correlation analysis (Fig. 7) revealed established relationships between surface properties. Increased water retention was associated with faster carbonation, resulting in lower surface pH value [48]. Interestingly, roughness was correlated with increased pH, likely due to the Expanded Clay surface which combines rough aggregate with smooth concrete areas. This combination of two separate materials may skew the results and limits its interpretive value. A minor negative correlation between pH

value and F_0-area was also observed, suggesting that lower pH values may support better microbial growth, in line with existing literature [18, 32].

While roughness is considered crucial for bioreceptivity [13, 18, 33], statistical data and correlation analysis in this study showed its effect on F_0-area was negligible. The limited porosity of Vinidur, despite its similar roughness to Textile, reinforces the conclusion that porosity plays a more critical role in supporting microbial attachment (Table 1). Previous studies have shown that surface structures matching the size of the microorganisms facilitate microbial attachment best [49–51]. The microalga used in this study is unicellular (cell size < 10 µm, data not shown), further confirming the materials capillary porosity has a bigger impact on algal attachment than the measured arithmetic roughness. As water retention is measured via capillary water uptake, it inherently reflects the capillary porosity of the surfaces crucial for microbial attachment. Although all samples were made from the same concrete mix and shared similar chemical composition, differences in surface structure led to varying biological growth outcomes, underscoring the influence of physical parameters on bioreceptivity.

This study highlights the complexity of bioreceptivity research, highlighting how even minor decisions in modeling biofilm formation on materials can significantly impact results, their relevance, and their applicability to real-world scenarios. Key factors such as material design, microorganism selection, inoculation methods, and the laboratory weathering set-up must be carefully considered to ensure they align with the research question.

5 Conclusion

The experimental set-up provided valuable insights into how concrete surface structure affects bioreceptivity, simulating real-world environmental conditions. The novel approach of an initial inoculation followed by a laboratory weathering experiment enabled accurate measurement of algal biomass attachment and growth instead of mere accumulation. The study highlights the importance of combining material properties, microorganism types, inoculation methods and laboratory weathering in bioreceptivity research. The use of Imaging PAM-F to monitor photosynthetic biofilms proved effective for low algal quantities, whereas the commonly used visual methods like high resolution surface imaging and colorimetry had limited utility. Adding the fungus *K. petricola* to the alga *Jaagichlorella* sp. increased complexity and led to a more representative and stable subaerial biofilm. The use of an alga/fungus combination enhanced the ecological relevance of the model, revealing synergistic effects that improved bioreceptivity assessments. This approach marks a significant step toward creating a uniform bioreceptivity test set-up that reflects natural complexity, offering more accurate and relevant results for future applications. Future research will be directed towards improving detection methods for early biofilm formation, including both photosynthetic and non-photosynthetic components, and investigating microbial-surface interactions in more detail using techniques such as scanning electron microscopy and staining of the extracellular polymeric substances produced by well-established biofilms. The use of complex multi-species biofilms will further refine bioreceptivity models and improve predictions of biofilm development in real-world applications.

Acknowledgements The authors would like to thank André Gardei for technical support.

Funding Open Access funding enabled and organized by Projekt DEAL. This study has been financed by the German Federal Institute for Materials Research and Testing (Bundesanstalt für Materialforschung und -prüfung) within the scope of the project MI 1642 Funktionsbeton, which also provided internal funding, as well as the Federal Ministry of Housing, Urban Development and Building (Zukunft Bau Forschungsförderung) under the Award Number 10.08.18.7–21.07_AbifFa.

Data availability Data sets generated during the study are available from the corresponding author on reasonable request.

Declarations

Conflict of interests The authors have no relevant financial or non-financial interests to disclose. The authors have no conflicts of interest to declare that are relevant to the content of this article. All authors certify that they have no affiliations with or involvement in any organization or entity with any financial interest or non-financial interest in the subject matter or materials discussed in this manuscript. The authors have no financial or proprietary interests in any material discussed in this article.

Appendix

See (Tables 4 and 5).

Table 4 Visual representation of F_0 chlorophyll fluorescence following 4 months of laboratory weathering. Data include all surface structures and replicates at high inoculation concentration for both the algae and algae- fungi inoculations. Growth patterns show high variability within a given combination of inoculation type and surface structure for Expanded Clay and Vinidur, as well as strong differences to each other and the surface structures Textile and Blanco

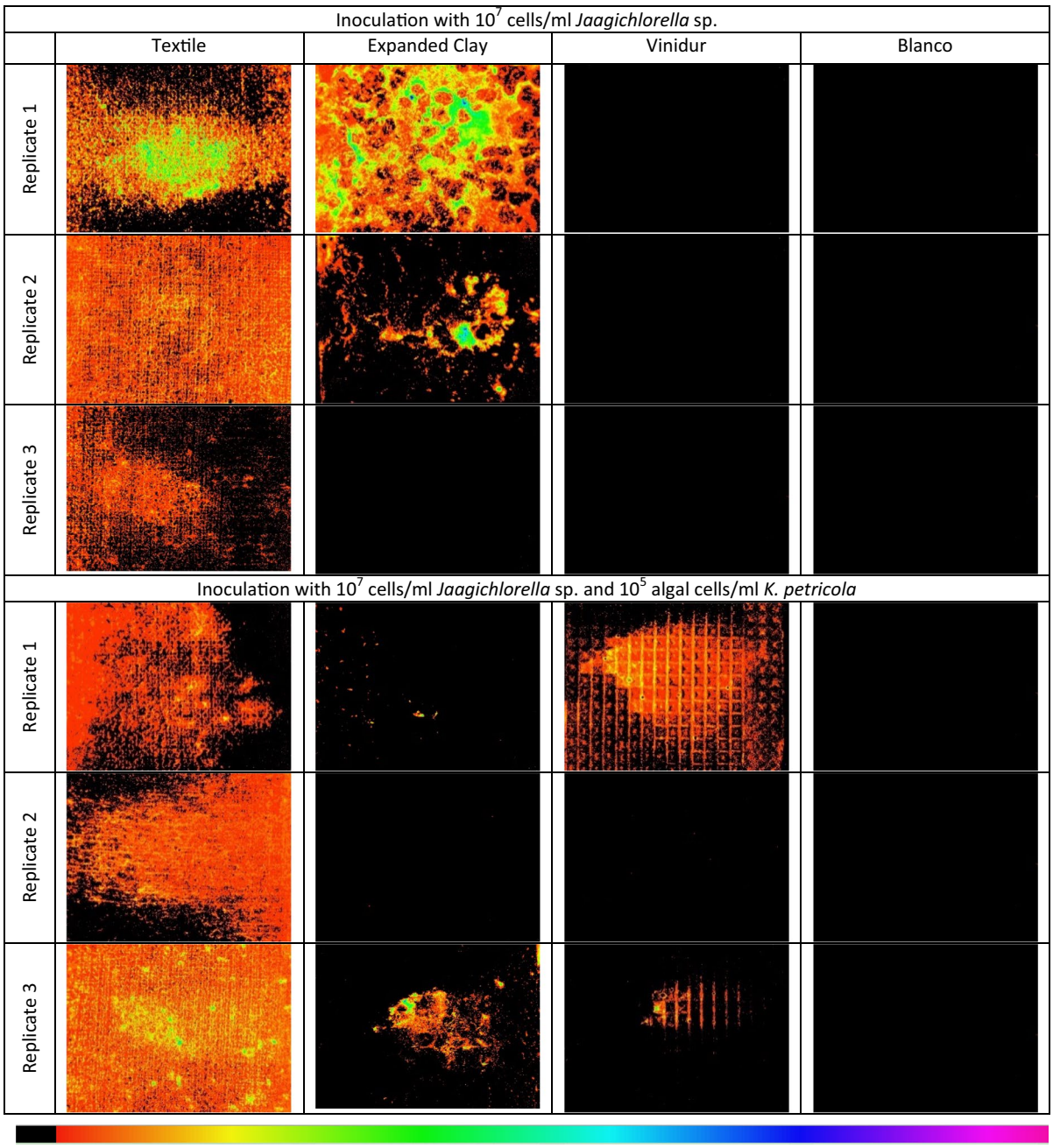

Table 5 Visual representation of F_0 chlorophyll fluorescence following 4 months of laboratory weathering. Data include all surface structures and replicates at low inoculation concentration for both the algae and algae- fungi inoculations. Growth patterns show high variability within a given combination of inoculation type and surface structure for Expanded Clay and Vinidur, as well as strong differences to each other and the surface structures Textile and Blanco

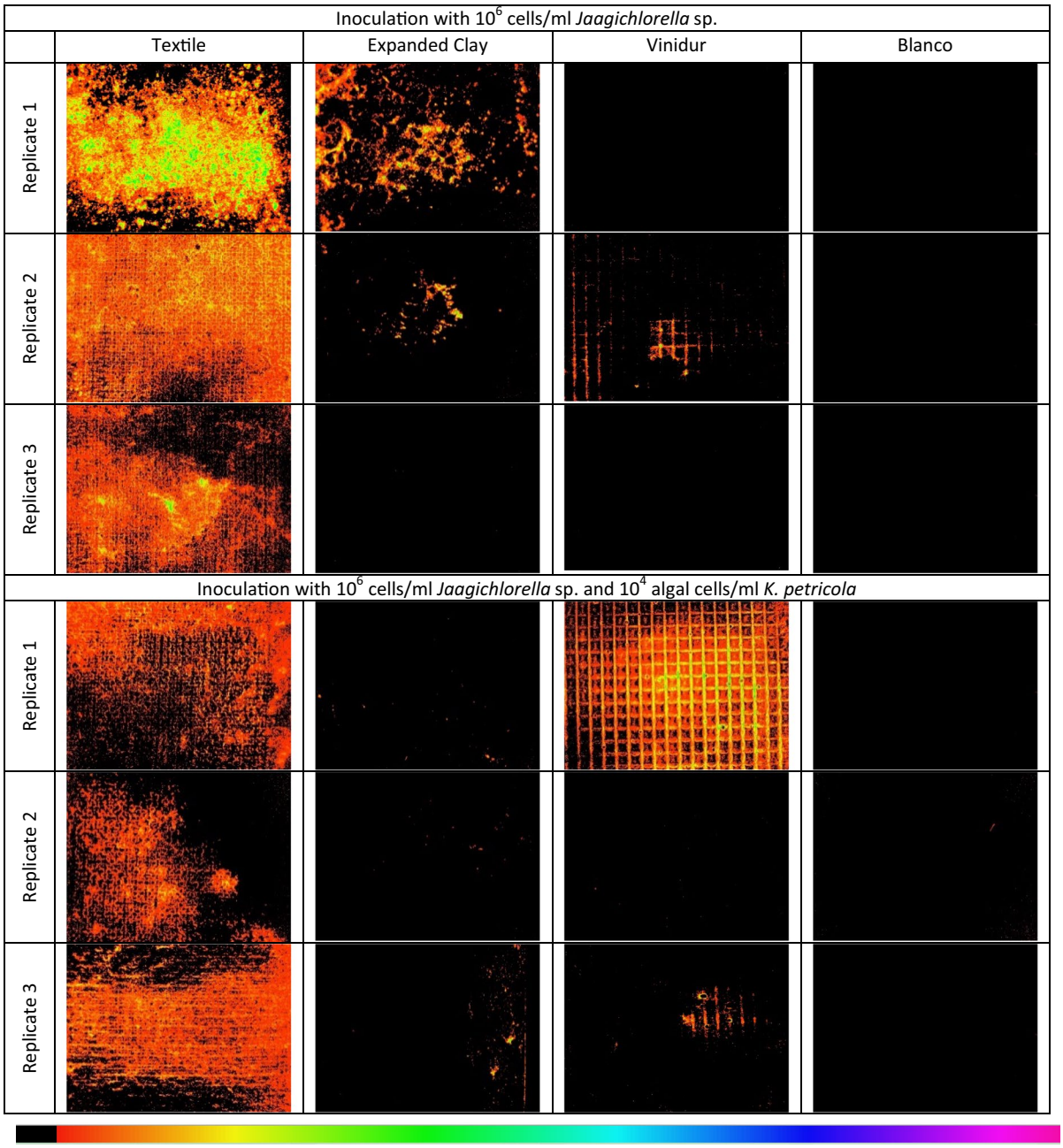

References

1. United Nations, World Urbanization Prospects: The 2018 Revision, United Nations, 2019. https://doi.org/10.18356/b9e995fe-en.
2. A. Aguinaga, Green Space: A Deficiency Affecting Public Health, (2018).
3. Veeger M, Ottelé M, Prieto A (2021) Making bioreceptive concrete: formulation and testing of bioreceptive concrete mixtures. J Build Eng 44:102545. https://doi.org/10.1016/j.jobe.2021.102545
4. Kondo MC, Fluehr JM, McKeon T, Branas CC (2018) Urban green space and its impact on human health. Int J Environ Res Public Health 15:445. https://doi.org/10.3390/ijerph15030445
5. Haahtela T, Bousquet J, Antó JM (2024) From biodiversity to nature deficiency in human health and disease. Porto Biomedical Journal 9:e245. https://doi.org/10.1097/j.pbj.0000000000000245
6. World Health Organization. Regional Office for Europe, Urban green spaces and health, World Health Organization Regional Office for Europe, Copenhagen, 2016. https://iris.who.int/handle/10665/345751.
7. Anguluri R, Narayanan P (2017) Role of green space in urban planning: outlook towards smart cities. Urban For Urban Green 25:58–65. https://doi.org/10.1016/j.ufug.2017.04.007
8. Gunawardena KR, Wells MJ, Kershaw T (2017) Utilising green and bluespace to mitigate urban heat island intensity. Sci Total Environ 584:1040–1055. https://doi.org/10.1016/j.scitotenv.2017.01.158
9. Halder B, Bandyopadhyay J, Al-Hilali AA, Ahmed AM, Falah MW, Abed SA, Falih KT, Khedher KM, Scholz M, Yaseen ZM (2022) Assessment of urban green space dynamics influencing the surface urban heat stress using advanced geospatial techniques. Agronomy 12:2129. https://doi.org/10.3390/agronomy12092129
10. Cavicchioli R, Ripple WJ, Timmis KN, Azam F, Bakken LR, Baylis M, Behrenfeld MJ, Boetius A, Boyd PW, Classen AT, Crowther TW, Danovaro R, Foreman CM, Huisman J, Hutchins DA, Jansson JK, Karl DM, Koskella B, Mark Welch DB, Martiny JBH, Moran MA, Orphan VJ, Reay DS, Remais JV, Rich VI, Singh BK, Stein LY, Stewart FJ, Sullivan MB, van Oppen MJH, Weaver SC, Webb EA, Webster NS (2019) Scientists' warning to humanity: microorganisms and climate change. Nat Rev Microbiol 17:569–586. https://doi.org/10.1038/s41579-019-0222-5
11. Manso M, Teotónio I, Silva CM, Cruz CO (2021) Green roof and green wall benefits and costs: a review of the quantitative evidence. Renew Sustain Energy Rev 135:110111. https://doi.org/10.1016/j.rser.2020.110111
12. Zhao J, Rao Q, Sun C, Ikram RMA, Fan C, Li J, Wang M, Zhang D (2024) A systematic review of the vertical green system for balancing ecology and urbanity. Water 16:1472. https://doi.org/10.3390/w16111472
13. S. Manso, Bioreceptivity Optimisation of Concrete Substratum to Stimulate Biological Colonisation, 2014.
14. H. Holger, Investigation of Building Materials Containing Algae-Prone Properties: Perspectives for Sustainable Façade Design, (2024). http://pea.lib.pte.hu/handle/pea/45105 (accessed November 20, 2024).
15. Gorbushina A (2007) Life on the rocks. Environ Microbiol 9:1613–1631. https://doi.org/10.1111/j.1462-2920.2007.01301.x
16. Gorbushina A, Broughton W (2009) Microbiology of the atmosphere-rock interface: how biological interactions and physical stresses modulate a sophisticated microbial ecosystem. Annu Rev Microbiol 63:431–450. https://doi.org/10.1146/annurev.micro.091208.073349
17. von Werder J, Venzmer H (2013) The potential of pulse amplitude modulation fluorometry for evaluating the resistance of building materials to algal growth. Int Biodeterior Biodegrad 84:227–235. https://doi.org/10.1016/j.ibiod.2012.03.009
18. Thu Hien T, Govin A, Guyonnet R, Grosseau P, Lors C, Garcia-Diaz E, Damidot D, Devès O, Ruot B (2012) Influence of the intrinsic characteristics of mortars on biofouling by Klebsormidium flaccidum. Int Biodeterior Biodegradation 70:31–39. https://doi.org/10.1016/j.ibiod.2011.10.017
19. Wiktor V, De Leo F, Urzì C, Guyonnet R, Grosseau Ph, Garcia-Diaz E (2009) Accelerated laboratory test to study fungal biodeterioration of cementitious matrix. Int Biodeterior Biodegrad 63:1061–1065. https://doi.org/10.1016/j.ibiod.2009.09.004
20. Łowińska-Kluge A, Horbik D, Zgoła-Grześkowiak A, Stanisz E, Górski Z (2017) A comprehensive study on the risk of biocorrosion of building materials. Corros Eng Sci Technol 52:13–21. https://doi.org/10.1080/1478422X.2016.1174326
21. Martinez T, Bertron A, Escadeillas G, Ringot E (2014) Algal growth inhibition on cement mortar: efficiency of water repellent and photocatalytic treatments under UV/VIS illumination. Int Biodeterior Biodegrad 89:115–125. https://doi.org/10.1016/j.ibiod.2014.01.018
22. Reiß F, Kiefer N, Noll M, Kalkhof S (2021) Application, release, ecotoxicological assessment of biocide in building materials and its soil microbial response. Ecotoxicol Environ Saf 224:112707. https://doi.org/10.1016/j.ecoenv.2021.112707
23. Sanmartín P, Miller A, Prieto B, Viles HA (2021) Revisiting and reanalysing the concept of bioreceptivity 25 years on. Sci Total Environ 770:145314. https://doi.org/10.1016/j.scitotenv.2021.145314
24. Guillitte O (1995) Bioreceptivity: a new concept for building ecology studies. Sci Total Environ 167:215–220. https://doi.org/10.1016/0048-9697(95)04582-L
25. Stohl L, Manninger T, Dehn F, von Werder J (2025) Understanding bioreceptivity of concrete: material design and characterization. Mater Struct 58:335. https://doi.org/10.1617/s11527-025-02863-y
26. Gaylarde C, Gaylarde P (2005) A comparative study of the major microbial biomass of biofilms on exteriors of buildings

in Europe and Latin America. Int Biodeterior Biodegrad 55:131–139. https://doi.org/10.1016/j.ibiod.2004.10.001
27. Barberousse H, Tell G, Yepremian C, Couté A (2006) Diversity of algae and cyanobacteria growing on building façades in France. Algol Stud 120:81–105. https://doi.org/10.1127/1864-1318/2006/0120-0081
28. Fuentes E, Vázquez-Nion D, Prieto B (2022) Laboratory development of subaerial biofilms commonly found on buildings. A methodological review, Building and Environment 223:109451. https://doi.org/10.1016/j.buildenv.2022.109451
29. Wiktor V, Grosseau P, Guyonnet R, Garcia-Diaz E, Lors C (2011) Accelerated weathering of cementitious matrix for the development of an accelerated laboratory test of biodeterioration. Mater Struct 44:623–640. https://doi.org/10.1617/s11527-010-9653-1
30. Urzì C, De Leo F (2007) Evaluation of the efficiency of water-repellent and biocide compounds against microbial colonization of mortars. Int Biodeterior Biodegrad 60:25–34. https://doi.org/10.1016/j.ibiod.2006.11.003
31. Escadeillas G, Bertron A, Ringot E, Blanc PJ, Dubosc A (2008) Accelerated testing of biological stain growth on external concrete walls. Part 2: Quantification of growths. Mater Struct 42:937. https://doi.org/10.1617/s11527-008-9433-3
32. Maury-Ramirez A, Muynck W, Stevens R, Demeestere K, De Belie N (2013) Titanium dioxide based strategies to prevent algal fouling on cementitious materials. Cement Concr Compos 36:93–100. https://doi.org/10.1016/j.cemconcomp.2012.08.030
33. De Muynck W, Ramirez AM, De Belie N, Verstraete W (2009) Evaluation of strategies to prevent algal fouling on white architectural and cellular concrete. Int Biodeterior Biodegrad 63:679–689. https://doi.org/10.1016/j.ibiod.2009.04.007
34. Eggert A, Häubner N, Klausch S, Karsten U, Schumann R (2006) Quantification of algal biofilms colonising building materials: chlorophyll a measured by PAM-fluorometry as a biomass parameter. Biofouling 22:79–90. https://doi.org/10.1080/08927010600579090
35. Nai C, Wong HY, Pannenbecker A, Broughton WJ, Benoit I, de Vries RP, Gueidan C, Gorbushina AA (2013) Nutritional physiology of a rock-inhabiting, model microcolonial fungus from an ancestral lineage of the Chaetothyriales (Ascomycetes). Fungal Genet Biol 56:54–66. https://doi.org/10.1016/j.fgb.2013.04.001
36. C. Nai, Rock-inhabiting fungi studied with the aid of the model black fungus Knufia petricola A95 and other related strains, (2014). https://doi.org/10.17169/refubium-10921.
37. Erdmann EA, Nitsche S, Gorbushina AA, Schumacher J (2022) Genetic engineering of the rock inhabitant knufia petricola provides insight into the biology of extremotolerant black fungi front. Fungal Biol. https://doi.org/10.3389/ffunb.2022.862429
38. Gorbushina AA, Beck A, Schulte A (2005) Microcolonial rock inhabiting fungi and lichen photobionts: evidence for mutualistic interactions. Mycol Res 109:1288–1296. https://doi.org/10.1017/S0953756205003631
39. Tonon C, Breitenbach R, Voigt O, Turci F, Gorbushina AA, Favero-Longo SE (2021) Hyphal morphology and substrate porosity -rather than melanization- drive penetration of black fungi into carbonate substrates. J Cult Heritage 48:244–253. https://doi.org/10.1016/j.culher.2020.11.003
40. R. Gerrits, richard wirth, A. Schreiber, N. Knabe, L. Benning, A. Gorbushina, High-resolution imaging of fungal biofilm-induced olivine weathering, Chemical Geology 559 (2020). https://doi.org/10.1016/j.chemgeo.2020.119902.
41. R. on the influence of biological deterioration Hofbauer, G. Gärtner, Microbial life on Façades, Springer Spektrum, 2021. https://doi.org/10.1007/978-3-662-54833-2.
42. Beysens D, Mongruel A, Acker K (2017) Urban dew and rain in Paris, France: occurrence and physico-chemical characteristics. Atmos Res 189:152–161. https://doi.org/10.1016/j.atmosres.2017.01.013
43. Kidron GJ, Temina M, Starinsky A (2011) An investigation of the role of water (rain and dew) in controlling the growth form of lichens on cobbles in the Negev Desert. Geomicrobiol J 28:335–346. https://doi.org/10.1080/01490451.2010.501707
44. Ulpiani G, di Perna C, Zinzi M (2020) Mist cooling in urban spaces: understanding the key factors behind the mitigation potential. Appl Therm Eng 178:115644. https://doi.org/10.1016/j.applthermaleng.2020.115644
45. Stohl L, Manninger T, von Werder J, Dehn F, Gorbushina A, Meng B (2023) Bioreceptivity of concrete: a review. J Build Eng 76:107201. https://doi.org/10.1016/j.jobe.2023.107201
46. A.A. Gorbushina, Idealbiofilm als neues Testsystem: Laborsimulation von Umwelteinflüssen und biologischer Einwirkung auf Materialien, in: Gesellschaft für Umweltsimulation e.V. Pfinztal : DWS Werbeagentur und Verlag GmbH, 2010: pp. 197–207.
47. Sterflinger K, Krumbein WE (1995) Multiple stress factors affecting growth of rock-inhabiting black fungi. Bot Acta 108:490–496. https://doi.org/10.1111/j.1438-8677.1995.tb00526.x
48. Šavija B, Luković M (2016) Carbonation of cement paste: understanding, challenges, and opportunities. Constr Build Mater 117:285–301. https://doi.org/10.1016/j.conbuildmat.2016.04.138
49. K. Ledwoch, G. Sai, O. Singh, Non-enclosure methods for non-suspended microalgae cultivation: Literature review and research needs, Renewable and Sustainable Energy Reviews 42 (2015). https://doi.org/10.1016/j.rser.2014.11.029.
50. Palmer J, Flint S, Brooks J (2007) Bacterial cell attachment, the beginning of a biofilm. J Ind Microbiol Biotechnol 34:577–588. https://doi.org/10.1007/s10295-007-0234-4
51. Miller AZ, Sanmartín P, Pereira-Pardo L, Dionísio A, Saiz-Jimenez C, Macedo MF, Prieto B (2012) Bioreceptivity of building stones: a review. Sci Total Environ 426:1–12. https://doi.org/10.1016/j.scitotenv.2012.03.026